



Innovative Lignin Nanoparticles: Biocontrol Agents against Garlic Crop Pathogen Fungi

Pooja Sharma^{1,2*} and Nivedita Sharma¹

¹Microbiology Laboratory, Dept. of Basic Sciences, Dr. Yashwant Singh Parmar University of Horticulture and Forestry, Nauni-Solan (Himachal Pradesh), India

²Department of Biological and Chemical Sciences, Baba Farid Colleges, Bathinda (Punjab), India
gunjanpu333@gmail.com

Available online at: www.isca.in, www.isca.me

Received 11th May 2024, revised 18th June 2024, accepted 30th June 2024

Abstract

By being employed for diverse applications by itself, lignin, which is thrown as waste during lignocellulosic biomass pre-treatments for the manufacture of biofuel, biogas, paper, and several other products, can greatly boost the economic viability of bio-refineries. We focused on discarded lignin and its usage in the synthesis of nanoparticles and their application as biocontrol agents for garlic crop. By fractionating agricultural waste biomass using the modified organosolv technique, lignin, which served as a capping agent for the synthesis of zinc oxide nanoparticles, was obtained and characterized using the Nuclear Magnetic Resonance (NMR) technique, whereas, the analytical investigations of lignin-derived zinc oxide nanoparticles (L-ZnO NPs) were carried out using the NMR, UV- Visible spectroscopy, Field Emission Scanning Electron Microscopy, and High Resolution Transmission Electron Microscopy techniques, which validated their production, morphology, shape, and size. The NPs were effective against 3 phyto-pathogenic fungi (Fusarium oxysporum, Fusarium proliferatum and Stemphylium vesicarium) that cause dry rot, basal rot, and blight of important cash crop- garlic (Allium sativum) in Himachal Pradesh, India. This was done in a lab setting before a net-house pot trial on garlic, where the L-ZnO NPs demonstrated strong antagonistic efficacy against the phyto-pathogenic fungi. Additionally, the environmentally friendly, cost-effective lignin-derivation from agricultural waste and subsequent lignin-mediated zinc oxide nanoparticle synthesis process would help in the production of numerous value-added materials in the future, as well as a potent antifungal agent for use in agriculture.

Keywords: Agricultural waste; Lignin; UV- Visible Spectroscopy; Zinc Oxide Nanoparticles; Biocontrol agent; NMR.

Introduction

Lignocellulosic biomass is derived from renewable natural resources or processes. Although it is primarily used for bioenergy, lignocellulosic biomass has received a lot of interest recently as a source for the creation of high-value compounds. The potential use of lignocellulosic biomass in the production of bio-chemicals, biofuels, biomaterials and other value added products is an important opportunity to minimize and valorise agroforest leftovers¹. Despite significant scientific and technological advances and investments to lessen environmental effect, the development of novel "green" biomass fractionation technologies has gained increasing interest from industry and governments².

If lignin is to be used as a feedstock for high-value products, it must be separated from the carbohydrates in the first phase of the bio-refinery chain. Organosolv pulping is one of the most effective pre-treatment techniques for meeting this criteria. From an environmental standpoint, the organosolv method fits several of the green manufacturing criteria³. As a result of the vast amounts of waste products accessible from agricultural lands, forestry, saw mills and pulp and paper mill activities, they are potentially significant resources⁴.

Nanotechnology is a rapidly developing scientific field with numerous applications in industries as diverse as agriculture and medicine. By utilising natural resources for the preservation, production, and protection of crops and livestock, nanotechnology can be used in agriculture. Numerous metallic nanoparticles have been successfully created using a variety of plant extracts and microorganisms, such as bacteria, fungus, viruses and microalgae⁵.

Zinc oxide nanoparticles (ZnO-NPs), for example, has been employed as an antifungal, antiviral and antibacterial agent⁶. Compared to other oxides, ZnO has attracted more interest since it is thought to be more environmentally friendly and biocompatible⁷.

Despite the fact that lignin and ZnO-NPs both have a growing number of agricultural applications, insufficient research has been undertaken on how these substances might interact in hybrid systems. To handle bacterial and fungal issues in crops, some research have hypothesized that lignin-mediated production of ZnO-NPs might be employed⁸. Since zinc functions as a micronutrient for plants, it has positive impacts on plant feeding, biomass development, and antioxidant barriers when ZnO-NPs are used to treat crops.

Three distinct kinds of plant pathogenic fungi *Fusarium oxysporum*, *Fusarium proliferatum* and *Stemphylium vesicarium* damage commercial crops like garlic, onions, wheat, barley, cotton, tomatoes and others by causing dry rot, basal rot and blight, which costs farmers who cultivate these products a living. Chemical control has negative effects on human and environmental health, and extensive resistance phenomenon make it difficult to apply fungicides continuously⁹.

As a result, the current study offers an environmentally friendly method for separating lignin from holo-cellulosic (Cellulose + Hemicellulose) agricultural waste, a biological method for producing effective ZnO-NPs using derived lignin as a stabilizing agent, and an evaluation of their impact on 3 challenging phyto-pathogenic fungi using a net house trial of garlic. ZnO-NPs are intriguing biomaterials because they have a large surface area, a long shelf life that is widely desired and, most importantly, a synergistic effect with potent antagonistic activity¹⁰. They are harmful to a wide variety of microorganisms, including bacteria and fungi, but biocompatible with human cells. Put another way, we take agricultural waste, partially transform it into a biocontrol agent and then utilise that agent to protect agricultural crops-a complete cycle.

Materials and Methods

Chemicals and Reagents: All of the reagents were of analytical purity and were used in this study without further purification. Chemicals needed for experimental work, including sodium hydroxide (NaOH), hydrogen peroxide (H₂O₂), sodium sulphide (Na₂S), sulfuric acid, formic acid, and acetic acid for the extraction of lignin from agricultural waste biomass and zinc acetate dihydrate (Zn(O₂CCH₃)₂) for the production of nanoparticles, were provided by Himedia Pvt. Ltd. in Mumbai, India and Merck, India Pvt. Ltd. The reactions were carried out with distilled water. To be used as test subjects for antifungal assays, IARI-New Delhi acquired three plant pathogenic fungi, *Fusarium oxysporum*, *Fusarium proliferatum*, and *Stemphylium vesicarium*, which, respectively, cause basal rot, Fusarium wilt, and Stemphylium blight diseases in commercial crops of garlic, onion, maize, tomato, wheat, beans and cotton were bought as sterile cultures.

Lignin Extraction : Wheat straw, rice straw, rice husk, corn stover and corn cob from agricultural regions in Nauni, Solan and neighbouring areas of Sirmaur, Himachal Pradesh, India, were gathered in clear plastic bags, cleaned, dried and ground to 2-3 mm sieve size and mixed in 1:1:1:1:1 ratio before being stored in airtight containers for use in subsequent experiments.

By utilizing an organic acid mixture and hydrogen peroxide, procedure given by Sharma et al., lignin was separated from the biomass¹¹. For this experiment, 25g of thoroughly mixed biomass was de-lignified with a solution of peroxy-formic acid/ peroxy-acetic acid (PFA/PAA), pulped with an 85% organic

acid mix (formic acid/acetic acid (FA/AA) ratio of 70:30 v/v and modified fiber/liquid ratio of 1:10) for 3-4h as minor modification of pulping duration and then bleached with H₂O₂ followed by lignin isolation. This procedure was repeated several times to remove the lignin entirely. The lignin in formic acid was precipitated by adding distilled water (5 times the volume of concentrated liquor), then filtering it through a Buchner funnel. The precipitate were then filtered using a Buchner funnel and washed thoroughly with distilled water. Finally, a 60°C oven was used to dry the precipitated lignin.

Characterization of Extracted Lignin Using NMR Analysis: NMR spectra were captured using a 400 MHz JEOLJNM ECS400 equipped with a z-gradient triple resonance probe at 25°C. Using the procedure described by Capanema et al. ¹³C NMR spectrum was obtained after dimethylsulfoxide (DMSO)-d₆ was used to dissolve 40mg of lignin¹². The pulse delay employed was 11 sec, which was 5 times longer than the lignin-carbon T₁ relaxation time. The precautions were taken that lignin to be free of impurities like extractives or carbohydrates and also to improve signal-to-noise ratio and reduce baseline and phasing distortions, the lignin/solvent solution was made concentrated as possible¹².

Green Synthesis of Nanoparticles using Lignin: For the formation of zinc oxide nanoparticles, 50ml of a 0.5M zinc acetate di-hydrate solution was made using distilled water. 1mL of aqueous lignin was added to the above mentioned solution after 10min of stirring¹³. A bright, white aqueous solution was generated *via* using 2.0 molar sodium hydroxide dropwise to maintain the pH at 12. It was then left in a magnetic stirrer for 2-3h. By using UV-Vis spectroscopy, the production of nanoparticles was verified. After centrifuging the light-coloured precipitates, the contaminants were repeatedly washed off using distilled water and then ethanol. A whitish powder of zinc oxide nanoparticles was created after spending the night drying at 60°C in the oven.

Characterization of Biosynthesized Nanoparticles: The UV-Visible Spectroscopy (UV-Vis), Field Emission Scanning Electron Microscopy (FESEM), High Resolution Transmission Electron Microscopy (HRTEM), and ¹H NMR techniques were used to characterise the biosynthesised Lignin-based Zinc Oxide Nanoparticles (L-ZnO NPs).

UV-Vis Spectroscopy: The optical characterization of produced lignin-based ZnO NPs was carried out using a UV-visible absorption spectrophotometer, which operated in the UV-visible wavelength range of 200 to 800 nm (Hitachi U-2800, Japan)¹⁰. To confirm the biogenic synthesis of lignin-based ZnO NPs, UV-visible spectroscopy investigation was done. The material was dissolved in deionized water for this standard analysis. The optical characterization of produced lignin-based ZnO NPs was carried out using a UV-visible absorption spectrophotometer, which operated in the UV-visible wavelength range of 200 to 800 nm (Hitachi U-2800, Japan).

Field Emission Scanning Electron Microscopy (FESEM):

The structure and surface morphology of the generated nanoparticles (L-ZnO NPs) were examined using the Field Emission Scanning Electron Microscopy (FESEM) (Model: SU8010 Series), Hitachi, Japan¹⁰. Due to the tendency of gas molecules to interfere with the electron beam and the secondary and backscattered electrons that are emitted and used for imaging, the operation was carried out under highly vacuum conditions. The microstructure image of the specimens in this study was taken using a Zeiss Crossbeam 340 in order to characterize them.

High Resolution Transmission Electron Microscopy (HRTEM):

L-ZnO NPs were imaged using a JEM 2100 PLUS, JEOL HRTEM model with a 200kV excitation voltage to ascertain the structure and properties of the biosynthesized nanoparticles¹⁰. A drop of the nanoparticle suspension was applied to a carbon-coated copper grid to prepare the grid for TEM investigation, and the water was then allowed to evaporate within a vacuum dryer. A transmission electron microscope was used to scan the grid of silver nanoparticles.

¹H-NMR Spectroscopy: At 25°C, 400 MHz JEOLJNM ECS400 outfitted with a z-gradient triple resonance probe was used to record NMR spectra. Dimethylsulfoxide (DMSO)-d₆ was used as a solvent to dissolve 40 mg of lignin based zinc oxide nanoparticles, and ¹H- NMR (Proton Nuclear Magnetic Resonance Spectroscopy) was performed¹⁴. A multinuclear NMR probe and a regular 5 mm NMR sample tube were utilized in all cases. With a single 15° pulse for quick relaxation, all measurements had been carried out at 298K and 500MHz resonance frequency for protons. Three seconds was the repeat time and about 20-80 scans were captured.

Efficacy of Biosynthesised L-ZnO NPs as Bio-controlling Agent:

With the purchase of plant pathogenic cultures of *Fusarium oxysporum* f. sp. *Ciceris* (Padwick) (ITCC NO. 7883), *Fusarium proliferatum* (Matsushima) Nirenberg (ITCC NO. 7095), and *Stemphylium vesicarium* (Wallr.) Wiltshire (ITCC NO. 6320) from IARI-New Delhi, in-vitro research was started. The strains were gathered, subcultured, and stocked on semi-solid potato dextrose agar plates¹⁵. Fresh cultures (7 days old) with complete plate growth were employed for further investigation.

Evaluation of Anti-Fungal Spectrum of LZnO NPs:

To ascertain the antagonistic capability of biologically produced nanoparticles against various pathogens, *in-vitro* studies were carried out by using 4 different concentrations of 0, 100, 300 and 500 ppm¹⁵. The fungus bit was sliced with a sterile borer and placed in the petri plate. The growth was observed for 7 days to assess effectiveness.

Application of ZnO NPs for Biocontrol of Garlic (*Allium sativum*):

Mass multiplication of pathogen¹⁶: Procedure from Turhan and Grosman was followed for production and mass

multiplication of fungal pathogens using corn and sand in the ratio of 3:1 (70g of corn and 30g sand) were used for the production of fungal inoculum. This culture was used for pathogen challenge of garlic seeds (*Allium sativum*)¹⁶.

Biocontrol experiment: The protective effect of most efficient synthesised L-ZnO nanoparticles were selected for studying the biocontrol in garlic plants inoculated with pathogenic fungus as per the treatment details given in Table-1 under net house conditions where soil and pots were prepared according to scientists¹⁶. The cultivated pathogens were added per pot one week before sowing of seeds. Garlic seeds cv. Solan Selection were soaked in 20 ml of synthesised ZnO NP solution for 1 h and then dried at room temperature. Seeds soaked in distilled water served as the control. Treated seeds were sown in pots containing potting mixture (1 seed/ pot). Cyclic replication of ZnO NP was done on the 7th and 15th day by spray method till 60 days' time period of trial.

Table-1: Details of the treatments applied to garlic trial.

Treatments	Description
T1(Control I)	Control (without Pathogen and LZnO NP)
T2 (Control II)	Pathogen 1
T3	Pathogen1+ LZnO NP
T4 (Control III)	Pathogen 2
T5	Pathogen 2+ LZnO NP
T6 (Control IV)	Pathogen 3
T7	Pathogen 3+ LZnO NP

Pathogen 1= *Fusarium oxysporum*, Pathogen 2= *Fusarium proliferatum*, Pathogen 3= *Stemphylium vesicarium*

Results and Discussion

Lignin Extraction and Characterization: By using the organosolv approach, it was possible to extract 20.32% of lignin from lignocellulosic agricultural waste biomass, together with 55.33% of residual cellulose (Table-2). In contrast, the untreated biomass revealed a content of 12.66% lignin and 35.61% holocellulose. Lignocellulosic biomass is comprised of cellulose, hemicellulose and lignin where hydrogen and Van der Waals bonds hold cellulose fibers to hemicellulose and lignin. It is a well-known fact that lignin severely restricts the ability of microbial enzymes to break down the polysaccharide components of plant cell walls, cellulose and hemicellulose^{17,18}. Therefore, pre-treatment of lignocellulosic is essential for the partial or complete removal of lignin if cellulose and hemicelluloses are to be fully exploited without losing too much sugar. Researchers have shown that a recently developed hybrid organosolv pre-treatment may successfully fractionate spruce biomass to produce pre-treated solids with high cellulose (72% w/w) and low lignin content (delignification up to 79.4% w/w). The high-purity lignin that was produced is appropriate for many cutting-edge applications¹⁹.

In a study similar to ours, after studying the effects of organosolv procedure on cocoa pod husks (CPH), Davidson et al. recovered and analyzed purified lignin and concluded several key aspects of developing a conceptual novel value chain from CPH²⁰. In another study, Sheng et al. used the organosolv method to extract lignin from low-cost or leftover sources in the agricultural industry.

The collected lignin samples were subjected to several analytical techniques in order to assess its molecular weight, thermal behavior, phenolic content and chemical structure²¹.

Table-2: Details of the treatment applied to agricultural mix biomass and comparison of untreated and organosolv treated biomass.

Waste Biomass	Untreated Biomass %		Organosolv Lignin Extraction %	
	Obtained Ligni	Residual Holo-cellulose	Obtained Lignin	Residual Holo-cellulose
Agricultural Mix Biomass	12.56	37.61	20.32%	55.33%

Using literature studies, the peaks for ¹³C-NMR spectroscopy were identified at 79.316, 78.992, 78.658, 39.709, 39.500 and 39.290ppm. These values were interpreted to indicate the presence of α , β and γ C, aliphatic C-O aromatic hydrogens, methoxyl groups (on Syringyl and Guaiacyl units) and aliphatic C-H, respectively. First, contaminants such as extractives or carbohydrates must be removed from the lignin sample (Figure-1).

Lignins can be identified, categorized, and their structural makeup determined using NMR spectroscopy. Aryl ether, condensed and uncondensed aromatic and aliphatic carbons are among the many structural details of lignin that can be revealed using the effective method of carbon (13)-NMR. Differences in functional group chemical shift between the two solvent systems are typically under 1ppm. Several prerequisites must be met for quantitative ¹³C-NMR analysis to be successful. The peaks were observed at 79.316, 78.992, 78.658, 39.709, 39.500 and 39.290 ppm, which indicated presence of α , β , γ -C, aliphatic C-O aromatic hydrogens, methoxyl groups (on Syringyl and Guaiacyl units), aliphatic C-H respectively. For phenolic compounds, bioenergy sources and functional materials, lignin is the most naturally plentiful source of aromatics.

This research focused on increasing lignin valorization by acid-catalyzed organosolv extraction. However, in the acidic environment, the majority of β -aryl ethers were cleaved to create C-C bonds. The incorporation of methanol as α -OCH₃ into lignin serves to avoid the cleavage of β -aryl ethers. In addition, 13C NMR spectroscopy demonstrated that acquired lignin was primarily separated through the cleavage of the related carbohydrates rather than the breakdown of β -aryl ether linkages²².

In a similar study, researchers found that the signals at 60 ppm and 56 ppm in the aliphatic area were attributed to methoxy and the C-C of β -O-4 bonds in lignin, respectively²³. For analysis with 13C NMR, milled wood lignin from Norway spruce and birch was prepared²⁴. The spectra of the spruce lignin showed essentially only guaiacyl units, while the birch lignin had about 40% guaiacyl and 60% syringyl units and aromatic units were primarily found to be assigned to syringyl C-2,6 and those between 110-115ppm were assigned to guaiacyl C-2. Tricker and his co-workers, processed lignin from organosolvand kraft pulping was analyzed using quantitative 13C-NMR spectroscopy, which allowed for the precise detection of various carbon species in the lignin structure. The aromatic and methoxy carbons were the only carbons in the NMR spectra that were subject to analysis. The aromatic region can also be broken down into aromatic carbons bonded to hydrogen (162–142 ppm), aromatic carbons bonded to carbon (142–125ppm) and aromatic carbons bonded to oxygen (162–142ppm) (125-102 ppm)²⁵.

A study found that depending on the kind of lignin, residual carbs ranged from 0.2 to 2.4 weight percent. Compared to organosolv lignin, alkaline lignin has a higher residual sugar content. These carbohydrates can come from polysaccharides that are still covalently bonded to lignin, as in the case of the Lignin-Carbohydrate Complex (LCC), or they can come from carbohydrates that become trapped during the precipitation process of lignin and then become non-covalently attached in the lignin following drying. According to earlier research, organosolv lignins have a higher purity²⁶.

Biosynthesis of L-ZnO NPs: The total lignin was further utilized to synthesize zinc oxide nanoparticles. Visual observation of the solution color change from brown to off-white predicted nanoparticle production which was confirmed by the peaks observed during UV-Vis spectroscopy (Figure- 2).

The obtained lignin was used to synthesize L-ZnO NPs. For holistic and cost-effective utilization of 2G biofuel, lignin derived from agricultural waste was used successfully to synthesize stable zinc oxide nanoparticles with unique shape and characteristics with an immense scope to be used in different important industries. The extracted lignin contains significant amounts of hydroxyl, methoxyl and carbonyl groups as provided by the characterization by NMR. Because of these functional groups, lignin can operate as a reducing agent to the zinc oxide nanoparticles. Functional groups found in lignin, such as phenolics and alkaloids, are responsible for capping, which enables it to contribute to the stability of nanoparticles. The synthesis of nanoparticles was validated after taking technical examination and in agreement with the literature. Researchers employed Agave-tequilana lignin to produce ZnO NPs and observed similar findings, including the creation of white nanoparticle powder²⁷. In the same year, similar findings were observed in a project to biosynthesize zinc oxide nanoparticles using the same approach¹³.

Characterization of L-ZnO NPs: Characterization of green generated L-ZnO NPs was carried out using a variety of techniques, including UV-Vis Spectroscopy to validate nanoparticle production by reduction of Zn^{2+} to ZnO and its absorption spectra as a measure to know about successful binding of the capping reagent (i.e., lignin in this study). While FESEM and HRTEM studies were carried out to determine the morphology, structure, and size of the synthesized L-ZnO NPs and they were in agreement with the other studies, ^1H NMR study was also carried out to learn about the functional groups showing in the nanoparticles¹¹.

UV-Vis Spectroscopy: By using UV-Vis spectroscopy of the colloidal solution in the region of 300-700 nm, the reduction of Zn^{2+} to ZnO was evaluated. According to the spectrum, the absorption range is between 297.059 and 359.071 nm (Figure-2). ZnO NPs synthesis were confirmed by the UV-Vis spectrum of the sample, which had a strong peaks at 270, 300, 320 and 360 nm, respectively, which is a hallmark of L-ZnO NPs¹⁷. Visual inspection of the reaction mixture provided the first indication that L-ZnO NPs had formed. This is demonstrated by the white NPs precipitates that have formed at the bottom of the flasks. The green-mediated synthesis was also examined while color changes in the suspension of the reaction were being observed. L-ZnO NPs were recovered from chemical and biological pathways and the resulting white powder was used for additional study. The immersion spectrum of the loaded ZnO nanoparticles with the absorption peak was found to be close to 360 nm in a study to manufacture ZnO NPs from coffee leaf extract²⁸, which is in agreement with the previously reported results.

The absence of any other distinguishing peaks in the spectrum supports the purity of the produced ZnO NPs. Due to the quantum size of the particles, the electronic transition from the valence band to the conduction band ($\text{O}2\text{p}$ to $\text{Zn}3\text{d}$ transition) is likely what caused the absorption peak at 341 nm. Due to the attachment of a substantially functionalized lignin matrix with several functional groups that can interact more with the nanoparticle surface, ZnO-NP and lignin's UV-visible absorption spectra exhibits a redshift when compared to pure ZnO NPs¹⁰.

Field Emission Scanning Electron Microscopy (FESEM): The sample produced by encapsulating ZnO NPs into the cavities provided by the lignin macromolecular matrix revealed highly equally dispersed nano-sized zinc oxide particles with a somewhat flake-like morphology. FESEM images of the synthesized ZnO NPs are shown in Figure-3(a-b). To analyze the form and surface appearance of the produced ZnO NPs, scanning electron microscopy was used to examine the nanoparticles. The voids created by the macromolecule aggregates were observed to contain the nanoparticles effectively dispersed, improving particle stability and preventing particle aggregation.

The majority of the ZnO NPs had an average diameter of between 50 and 60nm, were massively hexagonal in form, and were at the nano-meter scale. Using the program ImageJ 1.45, the size distribution of ZnO nanoparticles was examined. Particle size was determined by measuring the particles in a random field of view. The ZnO NPs were also considerably aggregated, which is a feature of green synthesis nanoparticles. This is due to the higher surface area of biosynthetic NPs and their long-term affinity, which leads to aggregation or agglomeration. It might be argued that ecological factors significantly affect NP stability and agglomeration. As a result, the NPs bind to one another and spontaneously form asymmetrical clusters during the production of nanoparticles²⁹. Similar results were found in various literatures using a green approach for synthesis of zinc oxide nanoparticles using lignin, in which nanoparticles dispersed in cavities formed by macromolecules and showed stability¹⁰.

High Resolution Transmission Electron Microscopy (HRTEM) Analysis: The shaft shape of the particles, which ranges in size from 50 to 60 nm and is more or less evenly distributed, was clearly visible in HRTEM images of zinc oxide nanoparticles trapped in macromolecule lignin clumps. The surface morphology, shape, and nano-size of the enclosed material were all retained¹⁰. After digitizing the multiple HRTEM pictures, the particle size was determined using the ImageJ software. The micrograph showed that although polyhedral morphology could also be seen, rod-shaped nanoparticles were more frequently found. The photos show that the particles tend to group together (Figure-4 a-b). HRTEM images of zinc-oxide nanoparticles entrapped in macromolecule lignin clumps demonstrated the particles' shaft morphology, which was more or less evenly distributed and ranged in size from 50 to 60 nm. The contained substance's nano-size, shape, and surface morphology were all preserved. The particle size was calculated using ImageJ software after digitizing the various HRTEM images. The important finding in this case was that the crystalline domain size obtained by examining HRTEM pictures closely matched the value discovered by XRD³⁰.

As a result, the environmentally friendly method of producing zinc oxide nanoparticles may be used to produce commodities with additional value and produce superior results. The high surface energy of nanoparticles may lead to particle aggregation. In a study on the preparation and analysis of zinc oxide nanoparticles (ZnO NPs), researchers also used TEM to examine the shape and particle size distribution of the ZnO NPs³¹. The TEM data can be used to determine the particles' irregular and spherical shapes³².

^1H NMR Spectroscopy: The ^1H NMR spectra of lignin based zinc oxide nanoparticles was obtained and studied. ^1H chemical shifts (δ) were measured in ppm, relative to TMS. The sharp peaks were obtained at 2.493, 2.497, 2.502, 2.506, 2.511 and 3.349 ppm which dedicate to the presence of methylene groups, protons attached to carbon molecules located in α -positions.

One of the finest ways to recognize hydrogen species and study their transport characteristics in ZnO is using ^1H NMR spectroscopy. By using ^1H NMR spectroscopy, the dynamical characteristics of mobile protons in the ZnO lattice site had previously been studied. Previous studies claimed that the mobile proton in the ZnO lattice was responsible for the NMR signal at 4.8ppm³³. The 2.49 and 2.50ppm peaks are in accordance with ^1H NMR spectra of lignin showing successful binding of lignin to ZnO NPs. The hydroxyl group was assigned to several NMR lines at or below 1ppm, and their diffusion characteristics were examined both before and after irradiation. This hydroxyl group's coupled jump diffusion after irradiation revealed a newly generated local structural disorder on the surface.

In earlier studies, a small NMR line at 4.1–4.8ppm, caused by mobile protons in the lattice site, was only seen in the sample synthesized at low temperature. Prior to radiation, the spectra showed several lines at 1ppm with a minor peak at 4.9 ppm, and the time-evolution showed that H1 and H2 had comparable relaxation times. Following irradiation, a smaller peak at 2.4ppm and an apparent narrow NMR line at 4.1ppm (H3) could be seen. ZnO nanoparticles' ^1H NMR spectra revealed peaks at 400 MHz, DMSO-d₆, 5.50ppm (H-2), 2.78 ppm (H-3), 3.26ppm (H-3), 6.14ppm (H-6), 6.12ppm (H-8), 4.97ppm (H-1''), 4.53ppm (H-1''') and 1.09ppm (3H, CH₃ of rhamnose), respectively³⁴.

In earlier studies, a small NMR line at 4.1–4.8ppm, caused by mobile protons in the lattice site, was only seen in the sample synthesized at low temperature. Prior to radiation, the spectra showed several lines at 1ppm with a minor peak at 4.9ppm and the time-evolution showed that H1 and H2 had comparable relaxation times. Following irradiation, a smaller peak at 2.4ppm and an apparent narrow NMR line at 4.1ppm (H3) could be seen¹⁴. According to another study, the peaks at 2.178 and 4.481 corresponded to the -OH groups for aliphatic and aromatic hydrocarbons, respectively³⁵.

Biosynthesized L-ZnO NPs as Bio-controlling Agent: *F. oxysporum*, *F. proliferatum* and *S. vesicarium* are 3 different species of plant pathogenic fungi damaging commercial crops such as garlic, onion, wheat, barley, cotton, tomato, and others, causing dry rot, basal rot and blight of crops leading to financial losses to the farmers who grow them for living. Chemical fungicides are known to linger in the environment and affect the ecology further. ZnO NPs have become an excellent bio-controlling agent alternative to conventional chemical and organic based medications or fungicides because of actions that specifically target and reduce toxicity¹¹.

The experiment's findings on lab scale were seen on petri-plates. It is easy to see how pathogen growth on concentrations of 100, 300, and 500ppm differs from pathogen growth on a control concentration of 0 ppm nanoparticles after 7 days of incubation at the proper temperature (Table-3).

The control of plant pathogenic fungi *F. oxysporum*, *F. proliferatum* and *S. vesicarium* were shown to be most effective at 500ppm concentration, according to the results.

Table-3: Antifungal activity of L-ZnO NPs against selected phyto-pathogens.

Fungal Pathogens	Diameter of colonies (in mm)			
	Control	100	300	500
<i>Fusarium oxysporum</i>	82	32	28	25
<i>Fusarium proliferatum</i>	90	40	26	22
<i>Stemphylium vesicarium</i>	85	33	25	17

The pot trial lasted 60 days (2 months), and the results are shown in the Figure-5 (a-g). From the sowing stage (day 0) to the post-harvesting stage (day 60), the plants displayed symptoms of dry rot and basal rot, as well as leaf drooping, which began approximately 15 days after sowing in the infected pots where the pathogens were inoculated before sowing, whereas pots with control plant and pathogen + nanoparticles combination displayed no symptoms and were healthy. In the infected pots, the harvested plants had parched stems and limited growth, as well as damped off leaves, whereas the control and nanoparticle treated plants were healthier and had more roots.

In the present study, the potent fungicidal action of ZnO NP-lignin conjugates greatly slowed the fungal pathogenic species' development. The encapsulation of ZnO NPs into the lignin core system boosts the nanoparticles' stability, allowing them to maintain their nanostructure and interact more effectively with pathogenic microbial strains, resulting in their inactivation. The inhibitory zone implies that zinc oxide nanoparticles have disrupted the fungal cell wall membrane. By offering unique locations for capturing the nanoparticles, macromolecular aggregates can efficiently stabilize zinc oxide nanoparticles, preventing particle aggregation and retaining them in nano-form^{11,36}. This is critical because the size and condition of the particles have a significant impact on the antimicrobial agent's specific action.

There is evidence that other studies on L ZnO NPs have produced results that are similar to those of the current work. *F. proliferatum* is a well-known plant pathogen that can cause illnesses in a range of key agricultural crops during the cropping season, including garlic, maize, wheat, barley, rice, asparagus, and pea, and is also involved in post-harvest garlic dry rot throughout crop growth³⁷.

In contrast, *F. oxysporum* is mostly responsible for basal plate rot in garlic, onion, maize, and other crops. Because chemical fungicides used to disrupt these infections cause environmental and health issues, these biosynthesized nanoparticles are a viable choice for use as a bio-controlling agent because they are environmentally safe and eradicate pathogens from crops³⁶.

In one study, ZnO nanoparticles were generated from *Azadirachta indica* leaf extract and tested for antifungal efficacy against phyto-pathogens before being compared to commercially available chemically synthesized ZnO nanoparticles (Chem-ZnO-NPs). The results for phytopathogens (*Alternaria alternata*, *Sclerotium rolfsii* and *Stemphylium solani*) revealed that *Azadirachta indica* mediated ZnO-NP was more effective than chemically generated ZnO-NP. As a result, the produced ZnO-NP can effectively replace commercially available fungal pesticides³⁷.

Researchers recently investigated the in vitro antifungal activity of ZnO in three forms of particles, including NPs with a size of 18 ± 2 nm, for three fungi: *F. oxysporum* f. sp. *lycopersici*, *Fusarium solani* (Mart.) Sacc. (Nectriaceae) and *Colletotrichum gloeosporioides* (Penz.) ZnO and ZnO NPs inhibited *F. solani* at the same concentration by 65% and 55%, respectively, and *C. gloeosporioides* at 60% and 59%. Different antifungal activity of ZnO NPs effective in interfering with the metabolism of phyto-pathogenic fungi was recently determined; it was observed that ZnO NPs at a concentration of 20 ppm were effective in inhibiting spore germination on *Bipolaris sorokiniana* (Pleosporaceae), at 10 ppm effective for *Alternaria brassicicola*³⁸.

ZnO nanoparticles inhibited *Fusarium oxysporum* mycelial growth and sporulation in vitro. Foliar spraying of ZnO NPs reduced the incidence and severity of *F. oxysporum* disease, allowing tomato plants to flourish. ZnO NPs have the potential to be applied as a bio-stimulant to enhance plant development and to prevent and control plant degeneration caused by phyto-pathogenic microorganisms^{39,40}.

Conclusion

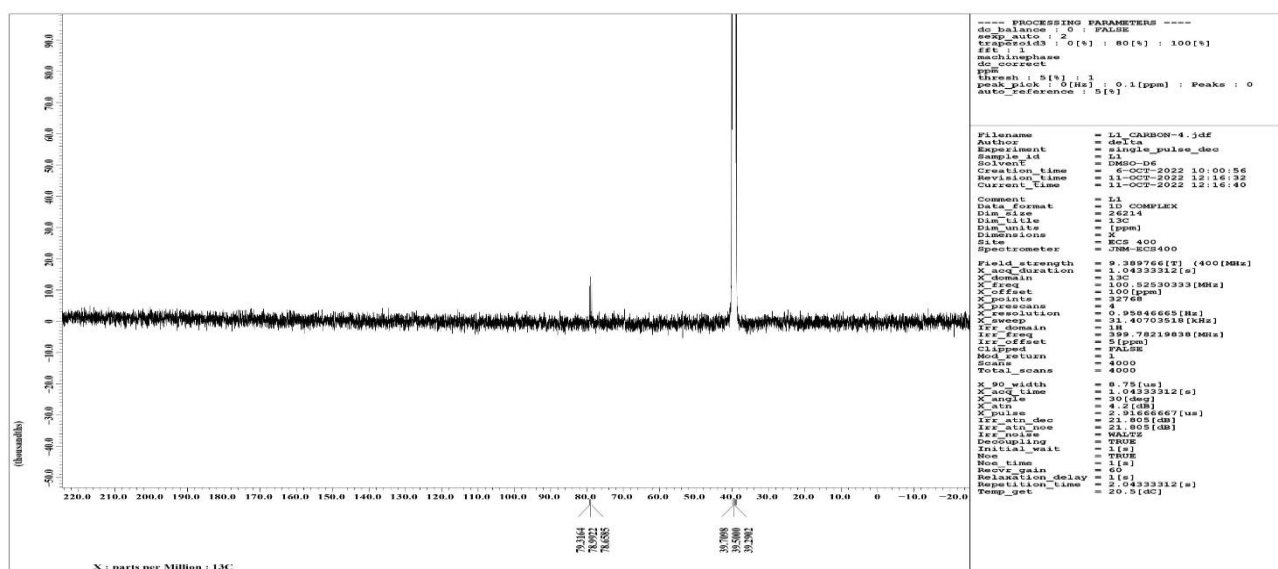


Figure-1: ¹³C- NMR spectra of organosolv lignin.

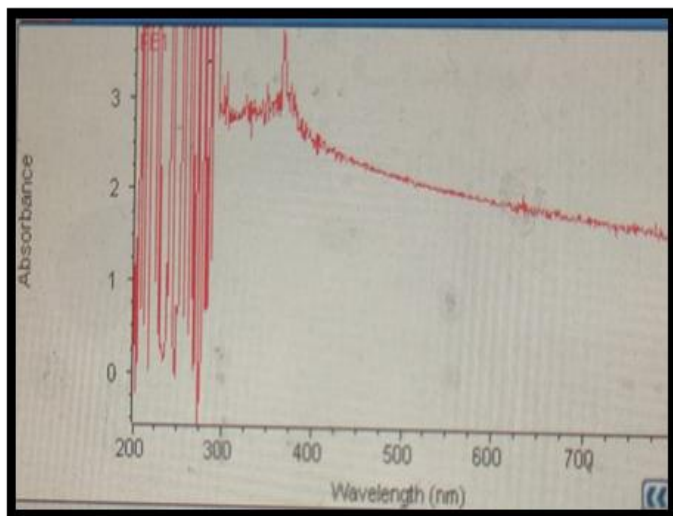


Figure-2: UV-Vis spectra of biosynthesized L-ZnO NPs.

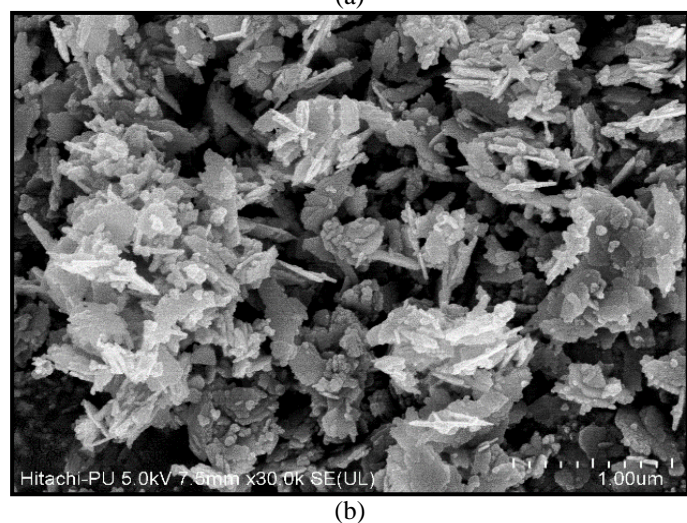
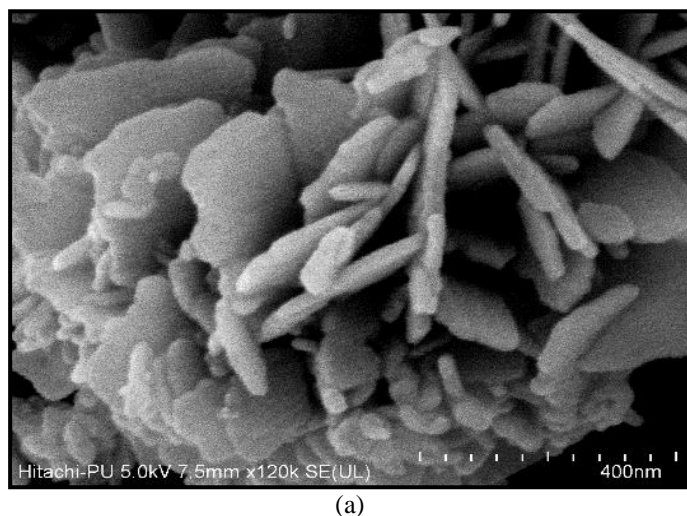


Figure-3: Field Emission Scanning Electron Microscopy (FESEM).

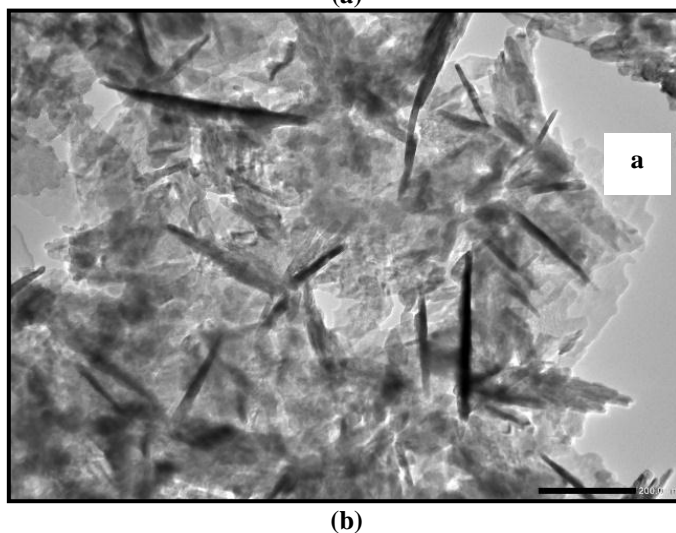
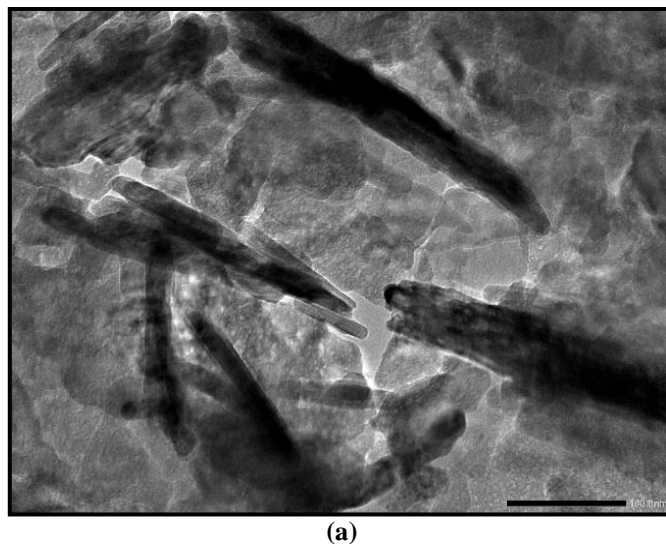


Figure-4: High Resolution Transmission Electron Microscopy (HRTEM) analysis.





Figure-5(a-g): Uprooted garlic plants after Day 60 of trial, showing biocontrol effect of L-ZnO NPs on roots and plant growth.

Acknowledgement

The NMR analysis was done by IIT Ropar and FTIR, FESEM and HRTEM were employed by SAIF laboratory, Panjab University, Chandigarh. Authors are grateful for their work towards current research.

References

1. Razo, I., Carrizales, L., Castro, J., Diaz, B.F. and Moroy, M. (2004). Arsenic and Heavy Metal Pollution of Soil, Water and Sediments in a semi-arid Climate Mining area in Mexico. *Water, Air, Soil and Pollution*, 152(1-4), 129-152.
2. Magalhães S., Filipe A., Melro E., Fernandes C., Vitorino C., Alves L., Romano A., Rasteiro M.G. and Medronho B. (2021) Lignin extraction from waste pine sawdust using a biomass derived binary solvent system. *Polymers* 13(7): 1090. <https://doi.org/10.3390/polym13071090>.
3. Nitsos C., Rova U. and Christakopoulos P. (2017) Organosolv fractionation of softwood biomass for biofuel and biorefinery applications. *Energies*, 11(1), 50. <https://doi.org/10.3390/en11010050>.
4. Thoresen P.P., Matsakas L., Rova U. and Christakopoulos P. (2020). Recent advances in organosolv fractionation: Towards biomass fractionation technology of the future. *Bioresource technology*, 306: 123189. <https://doi.org/10.1016/j.biortech.2020.123189>.
5. Stigsson C., Furusjö E. and Börjesson P. (2022). A model of an integrated hydrothermal liquefaction, gasification and Fischer-Tropsch synthesis process for converting lignocellulosic forest residues into hydrocarbons. *Bioresource Technology*, 353, 126070. <https://doi.org/10.1016/j.biortech.2021.126070>.
6. Del Buono D, Luzi F, Tolisano C, Puglia D and Di Michele A (2022). Synthesis of a lignin/zinc oxide hybrid nanoparticles system and its application by nano-priming in maize. *Nanomaterials*, 12(3), 568. <https://doi.org/10.3390/nano12030568>.
7. Chandrasekaran S., Anusuya S. and Anbazhagan V. (2022). Anticancer, anti-diabetic, antimicrobial activity of zinc

- oxide nanoparticles: A comparative analysis. *Journal of Molecular Structure*, 1263, 133139. <https://doi.org/10.1016/j.molstruc.2022.133139>.
8. Gomathi R and Suhana H (2021). Green synthesis, characterisation and antimicrobial activity of zinc oxide nanoparticles using *Artemisia pallens* plant extract. *Inorganic and Nano-Metal Chemistry*, 51(12), 1663-72. <https://doi.org/10.1080/24701556.2020.1852256>.
 9. Samb-Joshi KM, Sethi YA, Ambalkar AA, Sonawane HB, Rasale SP, Panmand RP, Patil R, Kale BB and Chaskar MG (2019). Lignin-mediated biosynthesis of ZnO and TiO₂ nanocomposites for enhanced antimicrobial activity. *Journal of Composites Science*, 3(3), 90. <https://doi.org/10.3390/jcs3030090>.
 10. Sardar M, Ahmed W, Al Ayoubi S, Nisa S, Bibi Y, Sabir M, Khan MM, Ahmed W and Qayyum A (2022). Fungicidal synergistic effect of biogenically synthesised zinc oxide and copper oxide nanoparticles against *Alternariacitri* causing citrus black rot disease. *Saudi journal of biological sciences*, 29(1), 88-95. <https://doi.org/10.1016/j.sjbs.2021.08.067>.
 11. Jose LM, Kuriakose S and Thomas S (2020). Fabrication, characterisation and in vitro antifungal property evaluation of biocompatible lignin-stabilized zinc oxide nanoparticles against selected pathogenic fungal strains. *BioNanoScience*, 10, 583-96. <https://doi.org/10.1007/s12668-020-00748-8>.
 12. Sharma P and Sharma N (2023). Lignin Derived from Forestry Biomass as Capping Reagent in the Biosynthesis and Characterisation of Zinc Oxide Nanoparticles and Their In Vitro Efficacy as a Strong Antifungal Biocontrolling Agent for Commercial Crops. *BioNanoSci.*, 13, 36-48. <https://doi.org/10.1007/s12668-022-01052-3>.
 13. Capanema EA, Balakshin MY, Chen CL, Gratzl JS and Gracz H (2001). Structural analysis of residual and technical lignins by 1H-13C correlation 2D NMR-spectroscopy. <https://doi.org/10.1515/HF.2001.050>.
 14. Yedurkar S, Maurya C and Mahanwar P (2016). Biosynthesis of zinc oxide nanoparticles using *Ixoracoccinea* leaf extract—a green approach. *Open Journal of Synthesis Theory and Applications*, 5(1), 1-4. <https://doi.org/10.1021/acssuschemeng.8b02234>.
 15. Park JK, Kwon HJ and Lee CE (2016). NMR Observation of mobile protons in proton-implanted ZnO nanorods. *Scientific reports*, 6(1), 1-8. <https://doi.org/10.1038/srep23378>.
 16. Ghadamgahi F, Mehraban SA and Shahidi BG (2014). Comparison of inhibitory effects of silver and zinc oxide nanoparticles on the growth of plant pathogenic bacteria. *International Journal of Advanced Biological and Biomedical Research*, 2(4), 1163-67.
 17. Sharma S, Sharma N and Sharma P (2022). Biosynthesis and Characterisation of Silver Nanoparticles Using Probiotic Strain *Lactobacillus Spicheri* G2 and Analysis of Its Antimicrobial Potential. *International Journal of Nanomaterials & Molecular Nanotechnology*, 4(1), 1-6. <https://doi.org/10.36266/IJNMN/125>.
 18. Abdelmigid HM, Hussien NA, Alyamani AA, Morsi MM, AlSufyani NM and Kadi HA (2022). Green synthesis of zinc oxide nanoparticles using pomegranate fruit peel and solid coffee grounds vs. chemical method of synthesis, with their biocompatibility and antibacterial properties investigation. *Molecules*, 27(4), 1236. <https://doi.org/10.3390/molecules27041236>.
 19. Arora A, Nandal P, Singh J and Verma ML (2020). Nanobiotechnological advancements in lignocellulosic biomass pretreatment. *Materials Science for Energy Technologies*, 3, 308-18. <https://doi.org/10.1016/j.mset.2019.12.003>.
 20. Matsakas L, Raghavendran V, Yakimenko O, Persson G, Olsson E, Rova U, Olsson L and Christakopoulos P (2019). Lignin-first biomass fractionation using a hybrid organosolv–Steam explosion pretreatment technology improves the saccharification and fermentability of spruce biomass. *Bioresource technology*, 273, 521-8. <https://doi.org/10.1016/j.biortech.2018.11.055>.
 21. Davidson DJ, Lu F, Faas L, Dawson DM, Warren GP, Panovic I, Montgomery JR, Ma X, Bosilkov BG, Slawin AM and Lebl T (2023). Organosolv Pretreatment of Cocoa Pod Husks: Isolation, Analysis, and Use of Lignin from an Abundant Waste Product. *ACS Sustainable Chemistry & Engineering*, 11(39), 14323-33. <https://doi.org/10.1021/acssuschemeng.2c03670>.
 22. Sheng Y, Ma Z, Wang X and Han Y (2022). Ethanol organosolv lignin from different agricultural residues: Toward basic structural units and antioxidant activity. *Food Chemistry*, 376, 131895. <https://doi.org/10.1016/j.foodchem.2021.131895>.
 23. Chen L, Liang Z, Zhang X, Zhang L, Wang S, Chen C, Zeng L and Min D (2022). A facile and novel lignin isolation procedure–Methanolic hydrochloric acid treatment at ambient temperature. *International Journal of Biological Macromolecules*, 222, 1423-32. <https://doi.org/10.1016/j.ijbiomac.2022.09.277>.
 24. Gan F, Cheng B, Jin Z, Dai Z, Wang B, Yang L and Jiang X (2021). Hierarchical porous biochar from plant-based biomass through selectively removing lignin carbon from biochar for enhanced removal of toluene. *Chemosphere*, 279, 130514. <https://doi.org/10.1016/j.chemosphere.2021.130514>.
 25. Zhang HM, Balakshin M, Capanema E, Gracz, H and Jameel H (2006). Quantification of lignin–carbohydrate linkages with high-resolution NMR spectroscopy. *Planta*, 233, 1097-1110.
 26. Tricker AW, Stellato MJ, Kwok TT, Kruyer NS, Wang Z,

- Nair S and Sievers C (2020). Similarities in recalcitrant structures of industrial non- kraft and kraft lignin. *Chemical Sustainable Chemical*, 10, 1002-1006.
27. Constant S, Wienk HL, Frissen AE, De Peinder P, Boelens R, Van Es DS, Grisel RJ, Weckhuysen BM, Huijgen WJ, Gosselink RJ and Bruijninx PC (2016). New insights into the structure and composition of technical lignins: A comparative characterisation study. *Green Chemistry* 18(9), 2651-65. <https://doi.org/10.1039/C5GC03043A>.
 28. Gutiérrez-Hernández JM, Escalante A, Murillo-Vázquez RN, Delgado E, González FJ and Toríz G (2016). Use of *Agave tequilana*-lignin and zinc oxide nanoparticles for skin photoprotection. *Journal of Photochemistry and Photobiology B: Biology*, 163, 156-61. <https://doi.org/10.1016/j.jphotobiol.2016.08.027>.
 29. Abel S, Tesfaye JL, Shanmugam R, Dwarampudi LP, Lamessa G, Nagaprasad N, Benti M and Krishnaraj R (2021). Green synthesis and characterisations of zinc oxide (ZnO) nanoparticles using aqueous leaf extracts of coffee (*Coffea arabica*) and its application in environmental toxicity reduction. *Journal of Nanomaterials*, 1-6. <https://doi.org/10.1155/2021/3413350>.
 30. Barzinjy AA and Azeez HH (2020). Green synthesis and characterisation of zinc oxide nanoparticles using *Eucalyptus globules* Labill. leaf extract and zinc nitrate hexahydrate salt. *SN Applied Science*, 2(5), 991. <https://doi.org/10.1007/s42452-020-2813-1>.
 31. Mahamuni PP, Patil PM, Dhanavade MJ, Badiger MV, Shadija PG, Lokhande AC and Bohara RA (2019). Synthesis and characterisation of zinc oxide nanoparticles by using polyol chemistry for their antimicrobial and antibiofilm activity. *Biochemistry and biophysics reports*, 17, 71-80. <https://doi.org/10.1016/j.bbrep.2018.11.007>.
 32. Muhammad W, Ullah N, Haroon M and Abbasi BH (2019). Optical, morphological and biological analysis of zinc oxide nanoparticles (ZnO NPs) using *Papaver somniferum* L. *RSC advances*, 9(51), 29541-8. <https://doi.org/10.1039/C9RA04424H>.
 33. Chaudhary A, Kumar N, Kumar R and Salar RK (2019). Antimicrobial activity of zinc oxide nanoparticles synthesised from *Aloe vera* peel extract. *SN Applied Sciences*, 1, 1-9.
 34. Wang Q, Chen K, Li J, Yang G, Liu S and Xu J (2011). The solubility of lignin from bagasse in a 1, 4-butanediol/water system. *BioResources*, 6(3), 3034-43.
 35. Attia GH, Moemen YS, Youns M, Ibrahim AM, Abdou R and El Raey MA (2021). Antiviral zinc oxide nanoparticles mediated by hesperidin and in silico comparison study between antiviral phenolics as anti-SARS-CoV-2. *Colloids and Surfaces B: Biointerfaces*, 203: 111724.
 36. Kavitha S, Dhamodaran M, Prasad R and Ganesan M (2017). Synthesis and characterisation of zinc oxide nanoparticles using terpenoid fractions of *Andrographis paniculata* leaves. *International Nano Letters*, 7, 141-7. <https://doi.org/10.1007/s40089-017-0207-1>.
 37. Mondani L, Chiusa G and Battilani P (2021). Fungi associated with garlic during the cropping season, with focus on *Fusarium proliferatum* and *F. oxysporum*. *Plant health progress*, 22(1), 37-46. <https://doi.org/10.1094/PHP-06-20-0054-RS>.
 38. Ali J, Mazumder JA, Perwez M and Sardar M (2021). Antimicrobial effect of ZnO nanoparticles synthesised by different methods against food borne pathogens and phytopathogens. *Materials Today: Proceedings*, 36, 609-15. <https://doi.org/10.1016/j.matpr.2020.03.173>.
 39. Kriti A, Ghatak A and Mandal N (2020). Inhibitory potential assessment of silver nanoparticle on phytopathogenic spores and mycelial growth of *Bipolaris sorokiniana* and *Alternaria brassicicola*. *Int. J. Curr. Microbiol. Appl. Sci.*, 9(3), 692-9. <https://doi.org/10.20546/ijcmas.2020.902.083>.
 40. González- Merino AM, Hernández- Juárez A, Betancourt- Galindo R, Ochoa- Fuentes YM, Valdez- Aguilar LA and Limón- Corona ML (2021). Antifungal activity of zinc oxide nanoparticles in *Fusarium oxysporum*- *Solanum lycopersicum* pathosystem under controlled conditions. *Journal of Phytopathology*, 169(9), 533-44. <https://doi.org/10.1111/jph.13023>.
 41. Sharma P, Thakur N, Mann NA and Umar A (2024). Melatonin as plant growth regulator in sustainable agriculture. *Scientia Horticulturae*, 323, 112421. <https://doi.org/10.1016/j.scienta.2023.112421>.